13th International Workshop on Wave Hindcasting and Forecasting
and 4th Coastal Hazards Symposium,
Banff, Canada Oct. 27 – Nov. 1, 2013

PROBABILITY OF OCCURRENCE OF ROGUE SEA STATES AND CONSEQUENCES FOR DESIGN

Elzbieta M. Bitner-Gregersen
Det Norske Veritas AS, DNV Research and Innovation
Veritasveien 1, NO-1322 Høvik, Norway
E-mail: elzbieta.bitner-gregersen@dnv.com

Alessandro Toffoli
Swinburne University of Technology
P.O. Box 218, Hawthorn, 3122 Vic., Australia
E-mail: alessandro.toffoli@gmail.com

1. INTRODUCTION

Current knowledge of ocean waves has significantly advanced in the last decade owing to many research efforts (see, e.g., Dysthe et al., 2008; Kharif et al., 2009) for a general overview). The occurrence of rogue waves, their mechanism, and detailed dynamic properties are now becoming clear and consistency between numerical models and experimental data has been documented by several researchers (e.g. Toffoli et al., 2010, 2013, Shemer et al., 2010). Despite these recent achievements, however, a full consensus on probability of occurrence of rogue waves has not been achieved yet, although some progress on the topic has been made recently. Such consensus, nonetheless, is essential for the evaluation of possible revision of offshore standards and classification society rules, which currently do not include rogue waves explicitly. This is because design practice is moving towards a more consistent probabilistic approach, where extremes are determined for a given return period (e.g. expected lifetime of a structure).

Probability of occurrence of rogue waves is related to mechanisms generating them. The recognised mechanisms responsible for occurrence of rogue waves can be classified as follows: linear Fourier superposition (frequency or angular linear focussing), wave–current interactions, crossing seas, quasi-resonance nonlinear interactions (modulational instability) and shallow water effects (Onorato et al. 2006a, 2006b, 2010, 2013; Toffoli et al., 2011, 2013; Didenkulova, 2010; Didenkulova and Pelinovsky, 2011; Sergeeva et al., 2011).

In the last decade most of the attention was given to the formation of rogue waves due to quasi-resonance nonlinear interactions referred to as modulational instability. It has been shown that the sea states responsible for occurrence of modulational instability in deep water are characterized by high steepness and a narrow wave spectrum, both in frequency and direction, and can be identified by the Benjamin Feir Index (BFI) (Onorato et al. 2001; Janssen 2003); such sea states can be addressed as *Rogue Sea States (M. Onorato, personal communication)*. The Benjamin-Feir Index, BFI is a measure of the relative importance of nonlinearity and dispersion. It can be defined as $BFI=(k_pH_s/2)/(\Delta\omega/\omega_p)$, where $k_pH_s/2$ is the wave steepness (k_p is the wavenumber at the spectral peak) and $\Delta\omega/\omega_p$ is the frequency spectral bandwidth ($\Delta\omega$ is the halfwidth at half-maximum of the spectrum and ω_p is the spectral peak frequency). Random waves are expected to become unstable when BFI=O(1), provided the wave field is unidirectional. It should be noted that the above definition of BFI is valid for stationary conditions *(A. Slunyaev, personal commu-nication).*

To investigate the frequency of occurrence of such *Rogue Sea States* in the North Atlantic, Bitner-Gregersen and Toffoli (2012) have used hindcast data from a few North Atlantic locations generated by Oceanweather Inc. and European Centre for Medium-Range Weather Forecast (ECMWF). The Oceanweather Inc. hindcast wind and wave covered the period 1988–1998 and were sampled every 3 h. They have been post-processed by Shell using the program APL Waves for the partitioning of 3-D spectra (i.e. directional wave spectra) into separate peaks. The ECMWF wind and wave data covered the period 2001–2009 and were archived at a sampling frequency of 6 h. Results revealed that such rogue-wave-prone sea states can actually occur in the North Atlantic, used as a wave design data base for ships, more often than once in the 20/25-yr period, the current design return period for ship structures. Also the highest sea state within the 10-yr time period analysed (H_s>15m) is characterised by $k_pH_s/2$=0.13, the conditions which may triggered the modulational instability. The findings of Bascheck and Imai (2011) support the above conclusions.

Onorato et al. (2006, 2010) have shown that the modulational instability of two crossing, identical, narrow-banded random wave systems can be responsible for the formation of rogue waves too. Such results have been confirmed through recent numerical simulations of the Euler equations and experimental work carried out at the MARINTEK Laboratories (Toffoli et al., 2011). Interestingly enough, such an unusual condition of two almost identical narrow banded spectra with high steepness and different direction was observed during the accident to the cruise ship Louis Majesty (Cavaleri et al, 2012).

The present study is investigating such rogue-wave-prone crossing seas and their probabilities of occurrence in the ocean. Hindcast data from the North Atlantic, the North and Norwegian Sea, off coast of Nigeria and Australia are used as the representation of the nature. Implications for design and operations of ship and offshore structures are discussed.

2. ROGUE WAVES IN CROSSING SEAS

The set of coupled Nonlinear Schrödinger (CNLS) equations

$$\frac{\partial A}{\partial t} - i\alpha\frac{\partial^2 A}{\partial x^2} + i(\xi|A|^2 + 2\varsigma|B|^2)A = 0 \qquad (1)$$

$$\frac{\partial B}{\partial t} - i\alpha\frac{\partial^2 B}{\partial x^2} + i(\xi|B|^2 + 2\varsigma|A|^2)B = 0 \qquad (2)$$

can describe the stability of a system of two non-collinear wave trains to the leading order in dispersion and nonlinearity (Roskes, 1976; Onorato et al., 2006; Shukla et al., 2006). *A* and *B* denote complex wave envelopes, α, ξ and ζ are coefficients (see Onorato et al., 2006, 2010 for details)

$$\alpha = \frac{\omega(\kappa)}{8\kappa^4}(2l - k^2) \qquad (3)$$

$$\xi = \frac{1}{2}\omega(\kappa)\kappa^2 \qquad (4)$$

$$\varsigma = \frac{\omega(\kappa)}{2\kappa}\left(\frac{k^5 - k^3l^2 - 3kl^4 - 2k^4\kappa + 2k^2l^2\kappa + 2l^4\kappa}{-2k^2 - 2l^2 + k\kappa}\right) \qquad (5)$$

where *(k, l)* and *(k, -l)* are the coordinates in Fourier space of the two carrier waves; $\omega = (g\kappa)^{1/2}$ with $\kappa = (k^2 + l^2)^{1/2}$.

To the leading order in nonlinearity, the surface elevation η(x, y, t) is related to the envelopes *A* and *B* in as follows:

$$\eta = \frac{1}{2}(Ae^{i(kx+ly-\omega t)} + Be^{i(kx-ly-\omega t)}) + c.c. \qquad (6)$$

where c.c. stands for complex conjugate and *g* is gravity acceleration. The angle between the two wave systems is defined as $\beta = 2\arctan(l/k)$. A linear stability analysis of plane wave solutions of Eqs.(1) and (2) (Ioualalen and Kharif, 1994; Badulin et al., 1995; Onorato et al., 2006b; Shukla et al., 2006) indicates that the growth rates of perturbations moving along the main direction of propagation depend not only on the length of the perturbation but also on the angle between the two wave systems. Growth rates different from zero have been found for $0<\beta<\arctan(2/2)^{1/2} \approx 70.53^o$. As β approaches $\beta_c \approx 70.53°$, the nonlinear terms in the coupled system become increasingly more important. Consequently, the ratio between nonlinearity and dispersion, a measure for the presence of extreme waves in single NLS (Onorato et al., 2001; Janssen, 2003), increases substantially (see Onorato et al., 2010). For $\beta > \beta_c$, however, the ratio changes sign and the coupled NLS change from focusing to defocusing. For random waves, larger deviations from Gaussian sea surface can be expected to occur already beginning for $\beta >$ 40° (Onorato et al., 2010). The growth rate decreases with increase of β and becomes zero for β approaching β_c. Therefore deviations from Normality should decrease for angle β close to 70.53^o.

These results have been confirmed through recent numerical simulations of the Euler equations carried out by the Higher Order Spectral Method (HOSM) proposed by West et al. (1987) and experimental work performed out in the MARINTEK Laboratories (Toffoli et al. 2011). The numerical simulations have been carried out to a third-order expansion so that the four-wave interaction is included (see Tanaka, 2001, 2007). The investigations have shown that the kurtosis, a measure of the probability of occurrence of extreme waves, depends on an angle β between the crossing wave systems. The maximum value of kurtosis is achieved for $40^o < \beta < 60^o$.

Crossing wave systems are often present at different locations in the ocean. They may represent wind sea and swell (or swells) or two or more swell components. It is easy to identify such wave systems by studying frequency-directional wave spectra, see Figure 1.

a)

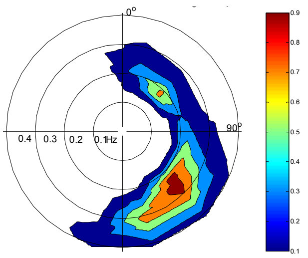

b)

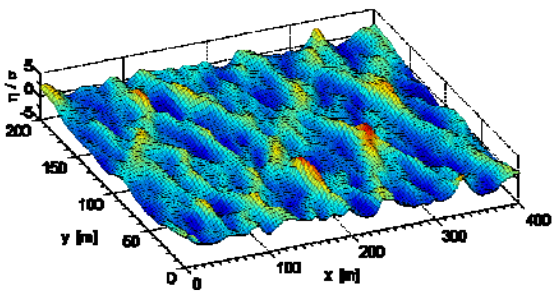

Figure 1. An example of the wave directional spectrum and sea surface when two wave systems are present. Numerical simulations were performed by HOSM.

3. HINDCAST DATA USED IN THE STUDY

Hindcast data provided by the Norwegian Meteorological Institute (met.no), ECMWF (European Centre for Medium-Range Weather Forecasts) and Oceanweather Inc. are used in the study. The data include the wind speed, the significant wave height and spectral peak period for the total sea, wind sea and swell as well as the mean wind speed, the mean and/or spectral peak direction for total sea, wind sea and swell.

Time series from the Norwegian database NORA10, generated by the 3G WAM model and developed at met.no with major support from a consortium of oil companies (The Norwegian Deep Water Programme), have been used in the study. The deep water North Atlantic location 59 ^{o}N, 12.0^{o}W (north-west of UK) is used in the analysis. The NORA10 data cover the period 1958-2009 and are sampled every 3 h. The NORA10 database validates better towards satellite and buoy observations than the ERA40 one from ECMWF (European Centre for Medium-Range Weather Forecasts).

The ECMWF ERA-Interim data used herein have been generated also by the 3G WAM model for the same North Atlantic location (59 ^{o}N, 12.0^{o}W) as the NORA10 data and cover the period 1989-2008. They are sampled every 6 h. The data have been received from met.no. In the considered North Atlantic location wind sea and swell is mostly always present.

Additionally, three locations, one in the Northern North Sea and two in the Norwegian Sea, are considered in the study: Statfjord (61.09^{o}N 1.40^{o}E), Halten (64.94^{o}N 7.98^{o}E) and Vøring (67.02^{o}N 6.93^{o}E) with the water depth ca. 150 m, 250 m and 1000 m, respectively. The data covering the period (1955-2000) were generated by the 2G WAM model by met.no and are sampled every 6 h. Simultaneous presence of wind sea and swell is also common for these three locations.

The Oceanweather Inc. hindcast data have been received from Shell. The data were generated by the Oceanweather wave model for three locations characterized by very different wave climate: NWS Australia, off coast of Nigeria and the Southern North Sea (SNS). At the Australia location both wind sea and swell is present. The SNS location is strongly dominated by wind-sea with very limited swells present, while in off coast of Nigeria primarily swells are present with a few significant wind-sea events. The original hindcast data have been post-processed by Shell by the program APL Waves, developed by the Applied Physics Department of John Hopkins University. The program divides 3D spectra (i.e., directional spectra) into separate peaks using Hanson and Phillips (2001) formulation. The method allows partitioning the frequency-direction spectrum into any number of wave components and this way separating wind-sea from swell components. For the data sets applied herein these wave components have then been recombined to finish with just two components per spectrum. The NWS Australia data were generated for the period 1994-2005 (water depth 250 m), the Nigeria data for the period 1985-1999 (water depth 1000 m), while Southern North Sea (SNS) for the period 1964-1995 (water depth 33 m). They were sampled every 3 hours for the Southern North Sea and Nigeria locations, while every hour for the NWS Australia one. Note that the Southern North Sea data include shallow water effects.

The hindcast data applied in the study represent sufficiently long time periods to provide satisfactory statistics of wave parameters and to indicate a possible occurrence of rogue-prone crossing sea.

4. OCCURRENCE OF ROGUE-PRONE CROSSING SEAS

In the present study we investigate frequency of occurrence of rouge-prone crossing seas in the selected ocean locations described in Sect.2, assuming that the hindcast data used in the analysis are good representation of the nature.

a)

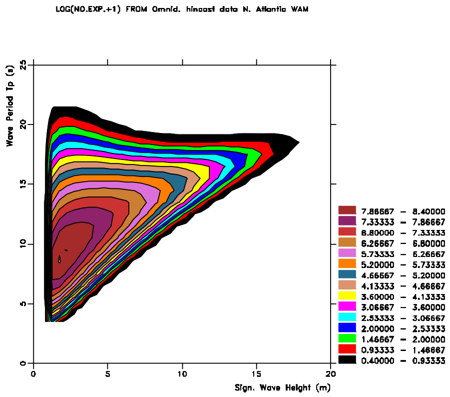

b)

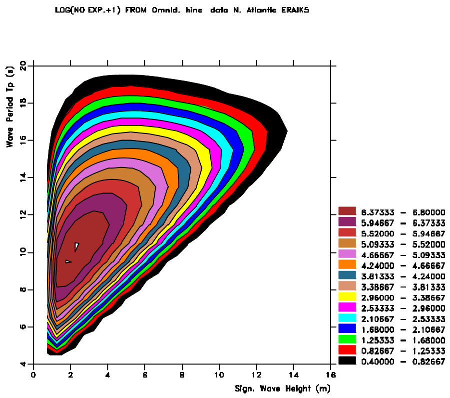

Figure 2. Contour plot of long term significant wave height H_{m0} and spectral peak period T_p for total sea, fitted model; a) NORA10 (1958-2009), b) ERA-Iterim (1989-2008).

The scatter diagrams of significant wave height H_{m0} and spectral peak period T_p for total sea, wind sea and swell have been established for the considered locations and fitted by a joint model; the 3-parameter Weibull distribution for H_{m0} and log-normal distribution conditional on H_{m0} for T_p (see Bitner-Gregersen, 2012, for details)

$$f_{H_s}(h_s) = \frac{\beta}{\alpha}\left(\frac{h_s-\gamma}{\alpha}\right)^{\beta-1} \exp\left\{-\left(\frac{h_s-\gamma}{\alpha}\right)^{\beta}\right\} \qquad (7)$$

where α is a scale parameter, β a shape parameter and γ a location parameter, and need to be estimated from data for the actual location.

$$f_{T_p|H_{m0}}(t_p \mid h_s) = \frac{1}{\sigma(h_{m0}) t_p \sqrt{2\pi}} \exp\left\{-\frac{(\ln t_p - \mu(h_{m0}))^2}{2\sigma(h_{m0})^2}\right\} \qquad (8)$$

where

$$\mu = \mathrm{E}(\ln T_p) = a_1 + a_2 h_{m0} \qquad (9)$$

$$\sigma = \mathrm{Std}(\ln T_p) = b_1 + b_2 e^{b_3 h_{m0}} \qquad (10)$$

the coefficients a_i, b_i, $i=1,2,3$ are estimated from data for the actual location. The model can also be applied for the zero-crossing wave period T_z (Tm_{02}). Examples of the fitted joint ($H_{m0,}$ T_p) model and empirical scatter diagrams are shown in Figure 2 and 3.

a)

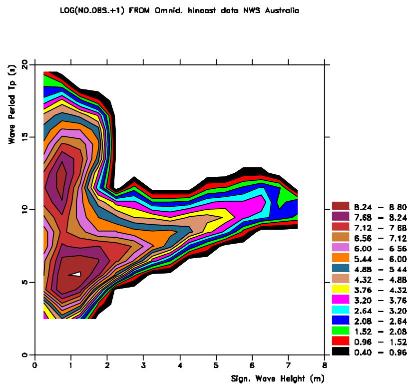

b)

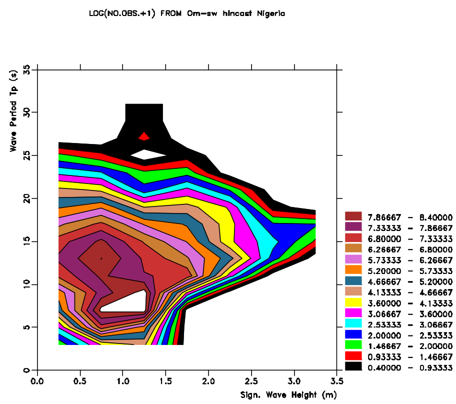

Figure 3. Contour plot of long term significant wave height H_{m0} and spectral peak period T_p for total sea; a) data from NWS Australia (1994-2005), Nigeria swell data (1985-1999).

The locations considered are characterized by different wave climate. At the North Atlantic, the Northern North Sea, the Norwegian Sea and the Australia locations wind sea and swell are present most of the time. However, in the North Atlantic, the Northern North and Norwegian Sea the scatter diagram of significant wave height and spectral peak period for total sea has one pronounced peak (see Figure 2) while the Australia data, due presence of long swell show two pronounced well separated peaks in the scatter diagram, one for wind-sea and one for swell (see Figure 3). The Southern North Sea is dominated strongly by wind-sea while off coast of Nigeria by swell with few wind sea components present. These location specific features of wave climate will influence joint environmental modelling and occurrence of rogue-prone crossing wave systems.

Occurrence of wind sea and swell having almost the same spectral period (Tp_w~Tp_s) and significant wave height (H_{sw}~H_{ss}) and crossing at the angle $40^o < \beta < 60^o$ is investigated for the considered locations. Figures 4 and 5 show results for the North Atlantic, Statfjord, Halten and Vøring.

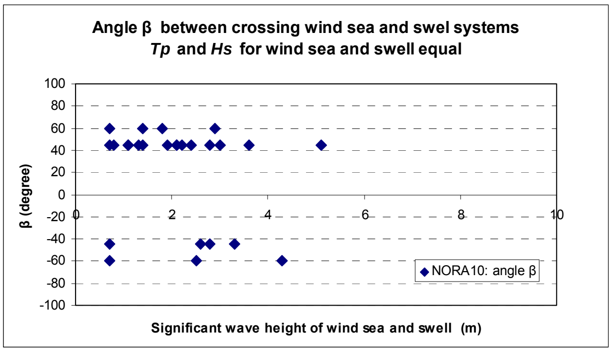

Figure 4. The angel between wind sea and swell having almost the same spectral period and significant wave height as a function of H_{sw} (H_{ss}). NORA10 data, the North Atlantic location.

Wind sea and swell crossing at the angle $40^o < \beta < 60^o$ and having almost the same spectral period (Tp_w~Tp_s) and significant wave height (H_{sw}~H_{ss}) are shown in Figure 4 as a function of H_{sw} (H_{ss}) for the North Atlantic location and NORA10 data (1958-2009). Such seas have been observed only for low and intermediate sea states with the total significant wave height $(2(H_{sw}^2 + H_{ss}^2))^{1/2}$ in the range 1.0-7.2 m and there are more of them for significant wave height lower than 2.5 m. Totally 27 crossing seas satisfying the significant wave height, spectral period and the angle β criteria have been identified. If the angle range is extended to $30^o < \beta < 60^o$ than wave systems with H_{sw}~H_{ss}=6.85 m (total H_{m0}=9.69 m) and the same spectral period Tp_w~Tp_s =14.9 s have been found but none sea states with H_{sw}>7 m.

The ERA-Iterim data available to the authors do not include the spectral peak period, only the zero-crossing wave period T_{m02}. Within this data set several wind sea and swell systems with the same significant wave height and crossing at the angle $40^o < \beta < 60^o$ have been found, again only for low and intermediate sea states.

Wind sea and swell systems satisfying the angle ($40^o < \beta < 60^o$), H_{sw}/H_{ss} and T_p criteria for Statfjord, Halten and Vøring are plotted in Figure 5. They include 56 crossing seas for Statfjord, 74 for Halten and 81 for Vøring; again majority of them are in low sea states and some in the intermediate sea states with the total significant wave height $(2(H_{sw}^2 + H_{ss}^2))^{1/2}$ in the range 0.4-7.2 m.

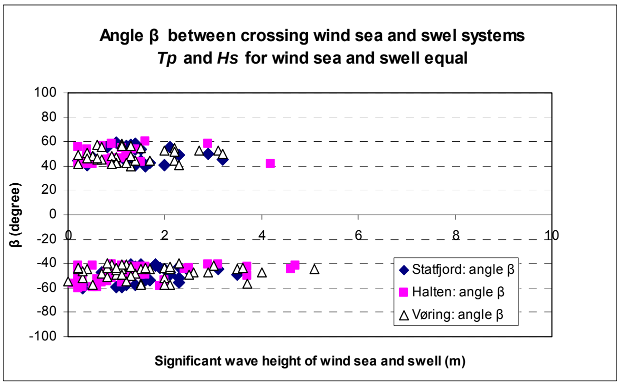

Figure 5. The angle between wind sea and swell having almost the same spectral period and significant wave height as a function of H_{sw} (H_{ss}). The Statfjord, Halten and Vøring locations.

As shown in Figure 3 at the Australia location wind sea and swell are well separated and the swell component has significantly longer periods than the wind sea component. Therefore none crossing rogue-prone wave systems have been found in this location. Similarly as at the Australia location, in off coast of Nigeria the swell has significantly different spectral periods than the wind sea and none crossing rogue-prone wave systems have been identified at this location. Such conditions could be present for different swell components; however, in the considered data set all swell components have been recombined in one swell component not allowing investigating different swell components separately. Again, rogue-prone crossing seas could be expected only in low and intermediate sea states; the highest swell in off coast of Nigeria has significant wave height in the range $3.0<H_{ss}<3.5$m.

The SNS location is strongly wind sea dominated and none rogue-prone crossing wave systems have been found in this location.

5. IMPLICATIONS FOR MARINE STRUCTURAL DESIGN AND OPERASTIONS

According to current design practice marine structural strength is evaluated for a given return period (i.e. a time period during which a hazard that can endanger the structure integrity appears not more than once). Ship structural strength and ship stability are calculated, following international standards, in extreme events with an occurrence of once in every 20/25-yr (Ultimate Limit State, ULS, in the structural reliability methodology). Offshore structures (including FPSOs: floating production storage and offloading units) follow a different approach to design of ship structures and are designed for the 100-yr return period (ULS). The Norwegian offshore standards (NORSOK, 2007) require that there must be enough space for the wave crest to pass beneath the deck to ensure that a 10 000-yr wave load does not endanger the structure integrity (Accidental Limit State, ALS). Knowledge about probability of occurrence of rogue waves is necessary for providing a consistent risk-based approach combining new information about extreme and rogue waves in a design perspective.

Visual observations of waves collected from ships in normal service (BMT, 1986) are currently used in the design of ship structures sailing world-wide. Four ocean areas in the North Atlantic, regarded as having the most severe wave climate, represent the wave base for ship design. The last significant wave height class in the design North Atlantic scatter diagram is in the range 16 – 17 m, IACS (2000).

Classification rules, in fact, permit the design of ships for restricted service (in terms of geographical zones and the maximum distance the ship will operate from a safe anchorage); in which case reduced design loads apply. Many aspects of the design, approval and operation require a detailed knowledge of local weather conditions. While in principle open to all ship types, the use of such restricted service is in practice mainly confined to high speed vessels.

Unlike ship structures, offshore structures normally operate at fixed locations and often represent a unique design. As a result, platform design and operational conditions need to be based on location specific met-ocean climate. Note that Floating Production Storage and Offloading (FPSO) systems are designed for the North Atlantic wave environment if location specific wave climate cannot be proved more appropriate.

The investigations carried out by Bitner-Gregersen and Toffoli (2012) based on the hindcast data from the few North Atlantic locations show that rogue-prone seas due to quasi-resonant interactions (modulational instability) can occur in low, intermediate and high sea states. This type of sea states can have impact on design loads and responses of marine structures depending on how frequent they can occur in the North Atlantic and in specific locations.

The present study indicates that rogue-prone crossing seas can be found only in low and intermediate sea states. Their occurrence depends on local wave climate features typical for a specific location. These rogue-prone sea states can be expected to impact operational conditions of marine structures but may also influence weather restricted design as well as design of local loads.

The accident that took place to the Louis Majesty ship in the Mediterranean Sea on March 3, 2010, is an example of rogue-prone crossing seas, Cavaleri et al. (2012). The ship was hit by a large wave that destroyed some windows at deck number five and caused two fatalities. Using the WAM wave model, driven by the COSMO-ME winds, a detailed hindcast of the local wave conditions has been performed. The results have revealed the presence of two comparable wave systems characterized by almost the same frequency (around 0.1Hz) and significant wave heights of approximately 3.5 m. The total significant wave height, H_{m0}, at the time of the accident was estimated around 5 m. These sea state conditions have been discussed by Cavaleri et al. (2012) in the framework of a system of two coupled Nonlinear Schrödinger (CNLS) equations, each of which describe the dynamics of a single spectral peak. Even though, due to the lack of measurements, it is impossible to establish the nature of the wave that caused the accident, it has been shown that the angle between the two wave systems during the accident is close to the condition for which the maximum amplitude of the breather solution is observed ($40^o < \beta < 60^o$).

6. CONCLUSIONS

The study points out that rogue-prone crossing wave systems responsible for generation of abnormal waves can occur primarily in low and intermediate sea states. Their occurrence is location specific, depending strongly on local features of wave climate. They are not expected to be present in the locations where wind sea and swell components, or several swell components, are well separated characterised by significantly different spectral peak periods.

These wave systems can be dangerous for marine structures depending on a type and size of a structure, as demonstrated by Cavaleri et al. (2012) for the cruise ship. They are expected to have most impact on operations of ships and offshore structures, but may also influence weather restricted design as well as design of local loads.

The investigations indicate that ships may experience such crossing wave systems more often than once during their life time. It should be noted that the present study is limited to the few locations only and do not include detail investigations of the identified crossing seas. Further research still is needed to reach firm conclusions.

Uncertainties of the data used in the study affect the presented results. They are due to the assumptions of the wave models applied for generation of the hindcast data, validation of the wave models as well as due to an approach adopted for estimation of wind sea and swell components. Further, it is assumed herein that the hindcast data approximate satisfactory the nature. The investigations of these uncertainties have been outside the scope of the analysis. However, is not expected that accounting for these uncertainties will change the present conclusions significantly.

Developments of warning criteria for rogue-prone crossing seas for marine structures are called for. This research has already been initiated by ECMWF, with which the EC EXTREME SEAS project has collaborated. Also Meteorological Offices are focusing on the topic. This work needs to continue to enhance safety at sea.

It is also important to be aware that change of storm tracks in some ocean regions, due to changing climate, may lead to secondary effects such as increase the frequency of occurrence of combined wave systems leading consequently to more frequent rogue events.

ACKNOWLEDGEMENTS
This work has been supported by the Norwegian Research Council project ExWaCli (the Project No. 226239) and the E.U. project EXTREME SEAS (SCP8-GA-2009-234175). The authors are indebted to met.no and Shell International Exploration and Production B.V. for providing the wave data. The authors thank Miguel Onorato and Alexey Slunyaev for fruitful discussions.

REFERENCES

Badulin, S. I., V. I. Shrira, C. Kharif, and M. Ioualalen, 1995: On two approaches to the problem of instability of short-crested water waves. *J. Fluid Mech*., 303, 297–326.

Bitner-Gregersen, E. M., 2012: Joint long-term models of met-ocean parameters. In: Guedes Soares C, editor. Marine technology and engineering: *CENTEC Anniversary Book*. vol. 1. CRC Press; 2012.

British Maritime Technology (Hogben, N. Da Cunha, L.F., and H.N. Oliver) 1986: *Global Wave Statistics*. Unwin Brothers Limited, London, England.

Cavaleri, L., L. Bertotti, L. Torrisi, E. Bitner-Gregersen, M. Serio, and M. Onorato. 2012: Rogue waves in crossing seas: The Louis Majesty accident. *J. Geophys. Res.*, 117, C00J10, doi:10.1029/2012JC007923.

Didenkulova, I., 2010: Shapes of freak waves in the coastal zone of the Baltic Sea (Tallinn Bay). *Boreal Env. Res*. 16.

Didenkulova, I. and E. Pelinovsky, 2011: Rogue waves in nonlinear hyperbolic systems (shallow-water framework), *Nonlinearity*, 24, R1-18.

Dysthe, K., H. E. Krogstad and P. Müller, 2008: Oceanic rogue waves. *Ann. Rev. Fluid Mech*., 40, 287-310.

Hanson, J. L., and O. M. Phillips, 2001: Automated Analysis of Ocean Surface Directional Wave Spectra. *J. Atmos. Ocean. Technol*., 18, pp. 277–29.

Hauser, D., K. K. Kahma, H. E. Krogstad, S. Lehner, J. Monbaliu and L. W. Wyatt (*Eds.*) 2005: Measuring and analysing the directional spectrum of ocean waves. Cost Office, Brussels.

Kharif, C., E. Pelinovsky and A. Slunyaev, 2009: Rogue waves in the ocean, *Advances in Geophysical and Environmental Mechanics and Mathematics*, Springer, Berlin.

IACS: 2000. IACS Rec. 34. Standard Wave Data. Rev.1, Corr. Nov. 2001.

Ioualalen, M., and C. Kharif, 1994: On the subharmonic instabilities of steadies three-dimensional deep water waves. *J. Fluid Mech*., 262, 265–291.

Janssen, P. A. E. M., 2003: Nonlinear four-wave interaction and freak waves. *J. Phys. Oceanogr*., 33, 863–884.

NORSOK, 2007: Standard N-003: Action and action effects, Norwegian Technology Standardization. Oslo, Norway.

Onorato, M., A. R. Osborne, M. Serio, and S. Bertone, 2001: Freak waves in random oceanic sea states. *Phys. Rev. Lett*., 86, 5831–5834.

Onorato, M., A. Osborne, M. Serio, L. Cavaleri, C., Brandini, C. Stansberg, 2006a: Extreme waves, modulational instability and second order theory: Wave flume experiments on irregular waves. *European J. of Mechanics B/Fluids*, 25, 586–601.

Onorato, M., A. Osborne, A. and M. Serio, 2006b: Modulation instability in crossing sea states: A possible mechanism for the formation of freak waves. *Phys. Rev. Lett.*, 96, 014503.

Onorato M., D. Proment, A. Toffoli, 2010.: Freak waves in crossing seas, *European Physical Journal*, 185, 45-55.

Onorato, M., S. Residori, U. Bortolozzo, A. Montina and F. T. Arecchi, 2013: Rogue waves and their generating mechanisms in different physical contexts. Physics Reports, 528, 47–89.

Osborne, A. R., 2010: *Nonlinear ocean waves and the inverse scattering transform.* International Geophysics Series, *Elsevie*r, San Diego.

Roskes, G. J., 1976: Nonlinear multiphase deep-water wavetrains. *Phys. Fluids,* 19, 1253–1254, doi:10.1063/1.861609.

Sergeeva, A., E. Pelinovsky and T. Talipova, 2011: Nonlinear random wave field in shallow water: variable Korteweg – de Vries framework. *Nat. Hazards Earth Syst. Sci*. 11, 323–330.

Shukla, P., I. Kourakis, B. Eliasson, M. Marklund, and L. Stenflo, 2006: Instability and evolution of nonlinearly interacting water waves. *Phys. Rev*. Lett., 97, 94501, doi:10.1103/PhysRevLett.97.094501.

Slunyaev, A. 2010: Freak wave events and the wave phase coherence. *Eur. Phys. J.* Special Topics, 185(1), 67-80.

Shemer, L., A. Sergeeva, A. Slunyaev, 2010: Applicability of envelope model equations for simulation of narrow-spectrum unidirectional random field evolution: experimental validation. *Phys. Fluids* 22, 016601. doi:10.1063/1.3290240.

Tanaka, M., 2001: Verification of Hasselmann's energy transfer among surface gravity waves by direct numerical simulations of primitive equations. *J. Fluid Mech.*, 444, 199-221.

Tanaka, M., 2007: On the role of resonant interactions in the short-term evolution of deep-water ocean spectra. *J. Physical Oceanography* 37, 1022–1036.

Toffoli, A., O. Gramstad, K. Trulsen, J. Monbaliu, E. M. Bitner-Gregersen and M. Onorato, 2010: Evolution of weakly nonlinear random directional waves: laboratory experiments and numerical simulations. *J. Fluid Mech*., 664, 313–336, 2010.

Toffoli A., E. M. Bitner-Gregersen, A. R. Osborne, M. Serio, J. Monbaliu, M. Onorato, 2011: Extreme waves in random crossing seas: Laboratory experiments and numerical simulations. *Geophys. Res. Lett*., 38, L06605, 5 pp. doi: 10.1029/201.

Toffoli, A., T. Waseda, H. Houtani, T. Kinoshita, K. Collins, D. Proment, M. Onorato, 2013: Excitation of rogue waves in a variable medium: An experimental study on the interaction of water waves and currents. *Phys. Rev*. E, 87, 051201(R).

West, B. J., K. A. Brueckner, R. S. Jand, D. M. Milder, and R. L. Milton, 1987: A new method for surface hydrodynamics. *J. Geophys. Res.*, 92, 11803–11824, 1987.